Although the derivations in this paper are given in terms of the magnetic field, the results are also valid for the electric field provided that dual quantities are substituted and the appropriate boundary conditions are added.

Acknowledgment

The author will be forever grateful to Prof. Silvester for the generous assistance received and the invaluable knowledge gained from him during the many years of association with him.

References

[1] A. Konrad, "Vector variational formulation of electromagnetic fields in anisotropic media," *IEEE Trans. Microwave Theory Tech.*, vol. MTT-24, pp. 553–559, Sept. 1976.
[2] W. J. English and F. J. Young, "An *E* vector variational formulation of the Maxwell equations for cylindrical waveguide problems," *IEEE Trans. Microwave Theory Tech.*, vol. MTT-19, pp. 40–46, Jan. 1971.
[3] G. O. Stone, "High-order finite elements for inhomogeneous acoustic guiding structures," *IEEE Trans. Microwave Theory Tech.*, vol. MTT-21, pp. 538–542, Aug. 1973.
[4] P. Silvester, "High-order polynomial triangular finite elements for potential problems," *Int. J. Eng. Sci.*, vol. 7, pp. 849–861, 1969.
[5] ——, "A general high-order finite element waveguide analysis program," *IEEE Trans. Microwave Theory Tech.*, vol. MTT-17, pp. 204–210, Apr. 1969.
[6] G. O. Stone, "Coupling matrices for high-order finite element analysis of acoustic-wave propagation," *Electron. Lett.*, vol. 8, pp. 466–468, Sept. 7, 1972.
[7] Z. J. Csendes and P. Silvester, "Numerical solution of dielectric loaded waveguides: I—Finite-element analysis," *IEEE Trans. Microwave Theory Tech.*, vol. MTT-18, pp. 1124–1131, Dec. 1970.
[8] Z. J. Csendes, "Solution of dielectric loaded waveguides by finite element methods," M.Eng. thesis, McGill Univ., Mar. 1970.
[9] P. Daly, "Hybrid-mode analysis of microstrip by finite-element methods," *IEEE Trans. Microwave Theory Tech.*, vol. MTT-19, pp. 19–25, Jan. 1971.
[10] ——, "Finite-element coupling matrices," *Electron. Lett.*, vol. 5, pp. 613–615, Nov. 27, 1969.
[11] B. Lax and K. J. Button, *Microwave Ferrites and Ferrimagnetics.* New York: McGraw-Hill, 1962.
[12] S. Ramo, J. R. Whinnery, and T. Van Duzer, *Fields and Waves in Communication Electronics.* New York: Wiley, 1967.
[13] F. E. Gardiol, "Computer analysis of latching phase shifters in rectangular waveguide," *IEEE Trans. Microwave Theory Tech.*, vol. MTT-21, pp. 57–61, Jan. 1973.
[14] S. F. Borg, *Matrix-Tensor Methods in Continuum Mechanics.* Princeton, NJ: D. Van Nostrand, 1963.
[15] A. Konrad, "Triangular finite elements for vector fields in electromagnetics," Ph.D. thesis, McGill Univ., Sept. 1974 (Thesis TC-24352, available from: National Library, Canadian Theses Division, 395 Wellington St., Ottawa, Ont., Canada, K1A 0N4.)
[16] A. Konrad and P. Silvester, "Triangular finite elements for the generalized Bessel equation of order *m*," *Int. J. Numer. Meth. Eng.*, vol. 7, pp. 43–55, 1973.
[17] A. Konrad, "Linear accelerator cavity field calculation by the finite element method," *IEEE Trans. Nucl. Sci.*, vol. NS-20, pp. 802–808, Feb. 1973.
[18] A. Konrad and P. Silvester, "A finite element program package for axisymmetric vector field problems," *Computer Physics Communications*, vol. 9, pp. 193–204, 1975.
[19] O. C. Zienkiewicz, *The Finite Element Method in Engineering Science.* New York: McGraw-Hill, 1971.
[20] G. C. Best, "Helpful formulas for integrating polynomials in three dimensions," *Math. Comp.*, vol. 18, pp. 310–312, 1964.
[21] P. Silvester and A. Konrad, "Axisymmetric triangular finite elements for the scalar Helmholtz equation," *Int. J. Numer. Meth. Eng.*, vol. 5, pp. 481–497, 1973.
[22] J. T. Oden, *Finite Elements of Nonlinear Continua.* New York: McGraw-Hill, 1972.

High-Azimuthal-Index Resonances in Ferrite MIC Disk Resonators

PIETRO DE SANTIS, MEMBER, IEEE

***Abstract*—This paper presents a study of the nonreciprocal high-azimuthal-index zero-radial-order modes which may resonate in ferrite MIC disk resonators magnetized perpendicularly to the ground plane. Both ferrite volume (FV) and edge-guided-wave (EGW) modes are investigated by using a suitable equivalent model. It is found that when the ferrite is saturated, a simple empirical parameter is sufficient to characterize the fringing-field effects at the disk's edge.**

I. Introduction

RECENTLY [1], [2], ferrite MIC disk resonators of large diameter have received some attention because they are suitable to study the propagation characteristics of the "edge-guided" waves (EGW) [3] in very much the same way as MIC ring resonators were used to study quasi-TEM propagation in isotropic MIC's.

Manuscript received May 28, 1976; revised November 5, 1976.

The author is with the Naval Research Laboratory, Washington, DC 20375, on leave from Selenia S.p.A., Rome, Italy, and the University of Naples, Naples, Italy.

Among the various modes which may resonate in such disk resonators, those appropriate to studying EGW characteristics are the $TM_{0,n,0}$ modes with $n = 4,5,6,\cdots$. These modes are TM with respect to the Z-axis, which is taken perpendicular to the ground plane. They present no nodes in the radial direction and are Z-independent.

An approximate analysis of a ferrite disk resonator magnetized perpendicularly to the ground plane was developed by the present author [4] using perfect magnetic-wall boundary conditions at the disk's edge. Subsequent experiments carried out by Brundle [2] measured EGW phase velocities 8 percent off the theoretical predictions.

The disagreement between theory and experiment was probably due to the use of unaccurate boundary conditions; i.e., to the neglect of fringing-field effects.

It is the purpose of this paper to study the fringing-field effects in ferrite MIC disk resonators and, more specifically, to evaluate how they affect the $TM_{0,n,0}$ resonances. The

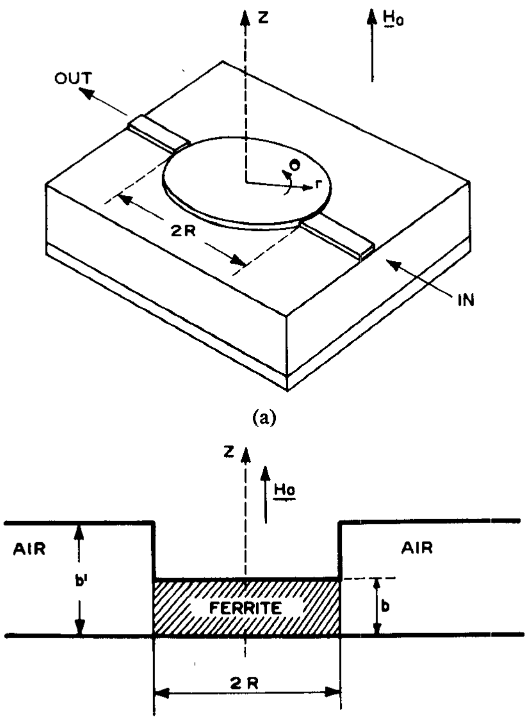

Fig. 1. (a) The MIC disk resonator on a ferrite substrate magnetized perpendicularly to the ground plane. (b) A radial cross section of the equivalent model.

study is based on an equivalent model which has been previously used to evaluate fringing-field effects in isotropic MIC's [5] and EGW in ferrite MIC's of semiinfinite width [1]. The details of the equivalent model are presented in the following section. Perhaps the most important feature of the equivalent model is that it is very simple and is semiempirical in character; i.e., it contains a "fringing-field parameter" b/b', to be determined by experiment.

The experimental determination of the fringing-field parameter is presented in Section III.

In Section IV the nature of the various resonances will be discussed. It will be shown that even if all the $TM_{0,n,0}$ modes have $E_Z(r)$ with no nodes in the radial direction, it is convenient to further subdivide them as belonging to two different groups: the EGW–$TM_{0,n,0}$ modes and the FV–$TM_{0,n,0}$ modes where FV stands for "ferrite volume."

"Transition points" will be identified on the mode chart of the resonator where the EGW modes transform into FV modes. The presence of these transition points will be shown to be due to the fringing fields at the disk's edge.

In Section V, it is shown how the knowledge of b/b' allows one to calculate the ratio between the reactive power stored in the fringing fields and the RF power contained in the ferrite volume under the strip conductor.

II. The Equivalent Model

In a previous work [1] the present author proposed an equivalent model to analyze the fringing fields associated with the EGW propagation in rectilinear microstrip lines of semiinfinite width. The analysis had a semiempirical character; i.e., it contained an empirical parameter to be determined by experiment.

The analysis was, in fact, based on the model used by Getsinger [5] for isotropic MIC's. Here we apply the same type of equivalent model to an MIC disk resonator.

Fig. 1 represents the actual structure (a) as well as a radial cross section of the approximate model (b). In the following it will be demonstrated that the ratio between the quantities b and b' indicated in Fig. 1(b) is a suitable parameter to characterize the fringing fields. The analysis of the equivalent model begins by recognizing that it is constituted of two radial waveguides of heights b and b' extending, respectively, for $0 < r < R$ and $r > R$, joined together at $r = R$.

As in Getsinger's analysis, the junction effects at $r = R$ are neglected because they greatly complicate the analysis and are not found necessary for practical results. Under these circumstances we assume Z-independent fields so that the total electromagnetic field in each waveguide can be represented as a superposition of pure $TE_Z \equiv (H_Z, E_\theta, E_r \neq 0)$ and $TM_Z \equiv (E_Z, H_\theta, H_r \neq 0)$ modes. Here we shall focus our attention on the TM_Z modes as they are the only ones affected by the magnetic anisotropy of the ferrite. We then associate to the TM_Z modes in each waveguide a radial transmission line of radial characteristic impedance [6]

$$Z_f = \frac{bE_{Zf}(r)}{2\pi r H_{\theta f}(r)} \tag{1}$$

$$Z_a = \frac{b'E_{Za}(r)}{2\pi r H_{\theta a}(r)}. \tag{2}$$

Here the subscripts f and a, respectively, indicate "ferrite" and "air." The various field components in (1) and (2) are calculated from Maxwell's equations in the usual manner (see, for example, [7]) and are repeated here for convenience. Within the ferrite, for $0 < r < R$, one finds

$$E_{Zf} = AJ_n(k_f r) \exp(\pm jn\theta) \tag{3}$$

$$H_{\theta f} = jAY\left[\pm \frac{n\mu_2}{\mu_1}\frac{J_n(k_f r)}{k_f r} - J_n'(k_f r)\right] \exp(\pm jn\theta) \tag{4}$$

$$H_{rf} = AY\left[\frac{\mu_2}{\mu_1} J_n'(k_f r) \mp \frac{n}{k_f r} J_n(k_f r)\right] \exp(\pm jn\theta) \tag{5}$$

with $k_f = (\omega/c)\sqrt{\varepsilon_f \mu_{\text{eff}}}$, $Y = Y_0\sqrt{\varepsilon_f/\mu_{\text{eff}}}$, and A is an amplitude factor, ω is the operation radian frequency, c is the velocity of light in vacuum, ε_f and μ_{eff} are the relative dielectric constant and effective magnetic permeability of the ferrite, μ_1 and μ_2 are the diagonal and off-diagonal entries of Polder's tensor, Y_0 is the characteristic admittance of vacuum, J_n is a Bessel function of the first kind, and the prime indicates differentiation with respect to the argument.

In air, for $r > R$, one finds

$$E_{Za} = BK_n(k_0 r) \exp(\pm jn\theta) \tag{6}$$

$$H_{\theta a} = -jBY_0 K_n'(k_0 r) \exp(\pm jn\theta) \tag{7}$$

$$H_{ra} = \mp \frac{BY_0 n}{k_0 r} K_n(k_0 r) \exp(\pm jn\theta) \tag{8}$$

where $k_0 = \omega/c$, B is an amplitude factor, and K_n a modified Bessel function of the second kind.

Let us now substitute the field components (3), (4), (6), and (7) into formulas (1) and (2) and impose the resonance condition

$$\overleftarrow{Z}_f(R) + \overrightarrow{Z}_a(R) = 0 \tag{9}$$

where $\overleftarrow{Z}_f = -Z_f$ and $\overrightarrow{Z}_a = Z_a$. Thus the characteristic equation of the model is found to be

$$X \frac{J_n'(X)}{J_n(X)} \mp n \frac{\mu_2}{\mu_1} = \frac{b}{b'} \mu_{\text{eff}} \zeta \frac{K_n'(\zeta)}{K_u(\zeta)} \tag{10}$$

with $X = k_f R$ and $\zeta = k_0 R$. Note that when $\mu_{\text{eff}} < 0$, k_f is an imaginary quantity and J_n must be replaced by the modified Bessel's function I_n.

In (10) the fringing-field parameter b/b' accounts for the fringing-field effects and must be determined by experimental techniques. The special cases $b/b' = 0$ and $b/b' = 1$, respectively, correspond to the widely used "perfect magnetic-wall" and "parallel-plate waveguide" models. The case $b/b' = 0$ corresponds to a short-circuited guiding edge, but is of no practical importance in a disk geometry.

As pointed out in [1], b/b' plays the same formal role as in Getsinger's analysis, and its practical utility is due to the fact that it can be easily determined by experiment, and it turns out to be a well-behaved, slowly varying function of such quantities as the applied dc magnetic field H_0, the radius of curvature R, and the operation frequency ω. In Section V it will be shown how b/b' is related to the fringing-field admittance as seen from inside the ferrite under the strip conductor and how, from this quantity, the reactive power stored in the fringing fields can be calculated.

III. The Determination of the Fringing-Field Parameter b/b'

The determination of b/b' is made by carrying out swept-frequency measurements of the transmission spectrum of the structure shown in Fig. 1(a) for different values of H_0.

In this manner, one measures the "mode chart" of the disk resonator. Fig. 2 is a typical mode chart representing the first ten azimuthally resonating $TM_{0,n,0}$ modes measured in a disk resonator with the following characteristics: diameter, 30 mm; thickness of the YIG substrate, 0.6 mm; $4\pi M_S = 1780$ Oe, $\varepsilon_f = 15$, $\Delta H_0 = 35$ Oe. In order to determine b/b', (10) was solved for H_0 as a function of the operation frequency $f = \omega/2\pi$. The azimuthal index n was given integer values from 1 to 10 and the parameter b/b' ranged from zero to one with $\Delta(b/b') = 0.1$.

Fig. 3 shows a family of curves which represent the solutions of (10) when $n = 6$ and $0 < b/b' < 1$. Similar curves were obtained for the other values of n.

When $H_0 < 4\pi M_S$, i.e., the YIG substrate is partially magnetized, the Green's tensor [8] was used in conjunction with a linear approximation [9] for the dependence of the ferrite's magnetization $4\pi M$ upon the applied magnetic bias H_0 (see the insert of Fig. 3). One relevant feature of the curves of Fig. 3 is the different algebraic sign of dH_0/df for $H_0 > 4\pi M_S$ and $H_0 < 4\pi M_S$. Such a phenomenon has been experimentally observed also in MIC ring resonators and spherical YIG resonators [9].

The determination of b/b' was achieved by superimposing the experimental points on the family of curves of Fig. 3. In this manner, at each point one could easily determine the numerical value of b/b' which would produce the best agreement between theory and experiment. What is shown in Fig. 3 for the $n = 6$ case, was repeated for n ranging from 4 to 10. An inspection of Fig. 3 immediately reveals that a single value of b/b' is not suitable to reproduce an experimental tuning curve. This is particularly true in the "unsaturated-ferrite" region $H_0 < 4\pi M_S$.

Therefore, the parameter b/b' must be a function of H_0 and f. Fig. 4 represents the behavior of b/b' as a function of H_0. It was derived by comparing the theoretical tuning curves with the experimental ones. In this figure one sees that for $n = 4,5,6$, i.e., for resonance frequencies between 4 and 8 GHz, the values of b/b' cluster in the vicinity of a curve whose equation was empirically found to be

$$\frac{b}{b'} = 1.7 \exp(-1.2H_0) + 0.27. \tag{11}$$

For $n = 8,9,10,11$, i.e., for frequencies between 8 and 12.5 GHz a better approximation was obtained by a curve of equation

$$\frac{b}{b'} = 1.4 \exp(-2.2H_0) + 0.5. \tag{12}$$

From these results, one can conclude that when the ferrite is saturated, i.e., $H_0 > 1.78$ kOe, b/b' is a slowly varying function of H_0, and constant values of 0.35 at C band and 0.5 at X band are good approximations to the actual situation.

Perhaps one important observation to be made at this point is that the behavior of b/b' as a function of H_0 for $H_0 < 1.78$ kOe depends upon the shape of the $4\pi M - H_0$ curve.

As long as the assumed linear dependence of $4\pi M$ on H_0 is an idealization of the actual physical situation, it is believed that the behavior of b/b' in Fig. 4 should be taken as a qualitative indication rather than providing quantitative information. However, to the author's knowledge, no exact information as yet exists on the behavior of $4\pi M$ as a function of H_0 within a ferrite substrate magnetized perpendicularly to its plane under conditions of partial magnetization.

IV. The Nature of the $TM_{0,n,0}$ Modes

In our experiments, the nature of the various resonances which appeared in the transmission spectrum of the resonator, was ascertained in the following manner. The TM character of the resonances was unambiguously recognized by the fact that they were H_0-dependent.

The Z-independence was assumed to be verified due to a diameter-to-substrate-thickness ratio of 50. The azimuthal index n was measured by means of an electric-field probe attached to a horizontal wheel above the substrate [2]. As far as the identification of the radial index was concerned, no problem existed when $\mu_{\text{eff}} < 0$. Under these circumstances $E_Z(r)$ within the ferrite is in fact proportional to a modified

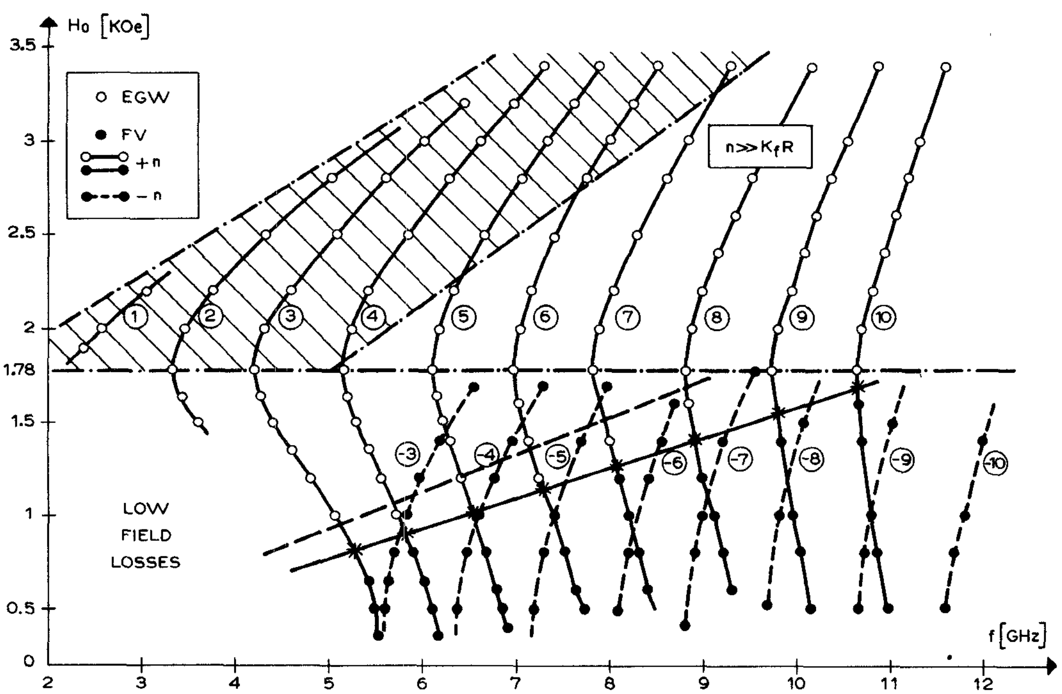

Fig. 2. Experimental $TM_{0,n,0}$ mode resonances in a ferrite MIC disk resonator. The continuous line with asterisks and the dashed line represent the transition-point locii, respectively, for $4\pi M = H_0$ and $4\pi M = (4\pi M_R/4\pi M_S)\cdot H_0$ ($H_0 \leq 4\pi M_S$).

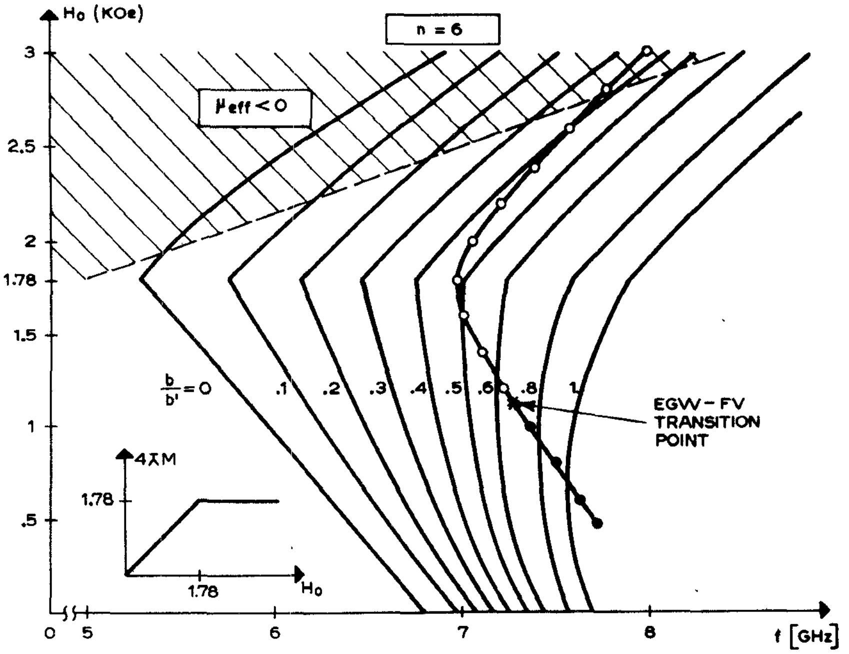

Fig. 3. Theoretical tuning curves for different values of $b/b' \cdot (n = 6)$. Open and solid circles are experimental points representing, respectively, EGW and FV $TM_{0,n,0}$ resonances.

Bessel function of the first kind which has no nodes. Therefore the radial index is zero. When $\mu_{\text{eff}} > 0$, however, $E_Z(r) \sim J_n(k_f r)$, which is an oscillatory function of its argument.

Under these circumstances, the value of $k_f R$ was calculated from the values of H_0 and f measured at each particular resonance. In any case, it was found $k_f R < p_{n1}$, where p_{n1} is the first root of J_n. This guaranteed that the azimuthal index was indeed zero.

It is on the occasion of calculating the values of $k_f R$ for each resonance under conditions of positive μ_{eff} that we recognized the need to distinguish between two types of $TM_{0,n,0}$ modes: the EGW–$TM_{0,n,0}$ modes and the FV–$TM_{0,n,0}$ modes. In the former type, $E_Z(r)$ is peaked at the disk's edge, while in the latter $E_Z(r)$ has a maximum at some point within the range $0 < r < R$.

From a mathematical point of view this is equivalent to saying that under conditions of positive μ_{eff}, EGW–

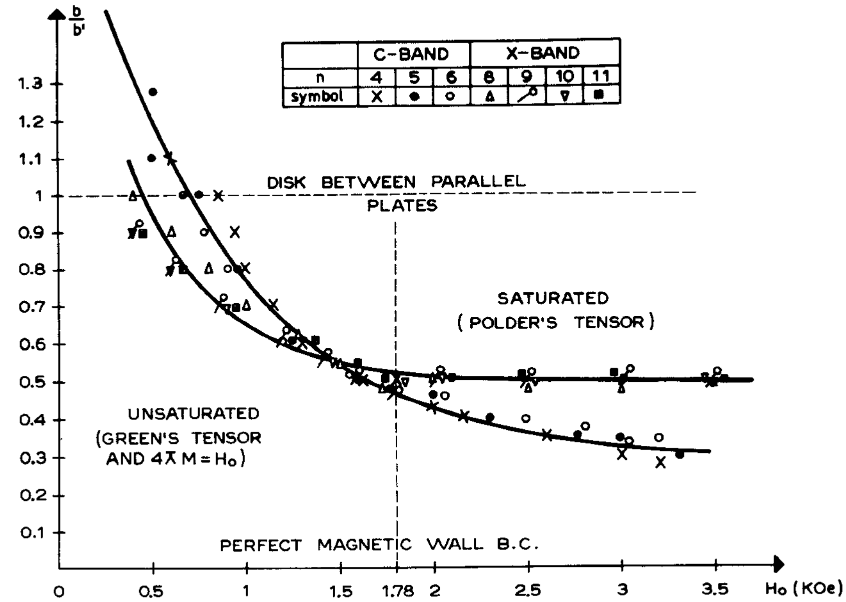

Fig. 4. Numerical values of b/b' as calculated from diagrams of the type shown in Fig. 3.

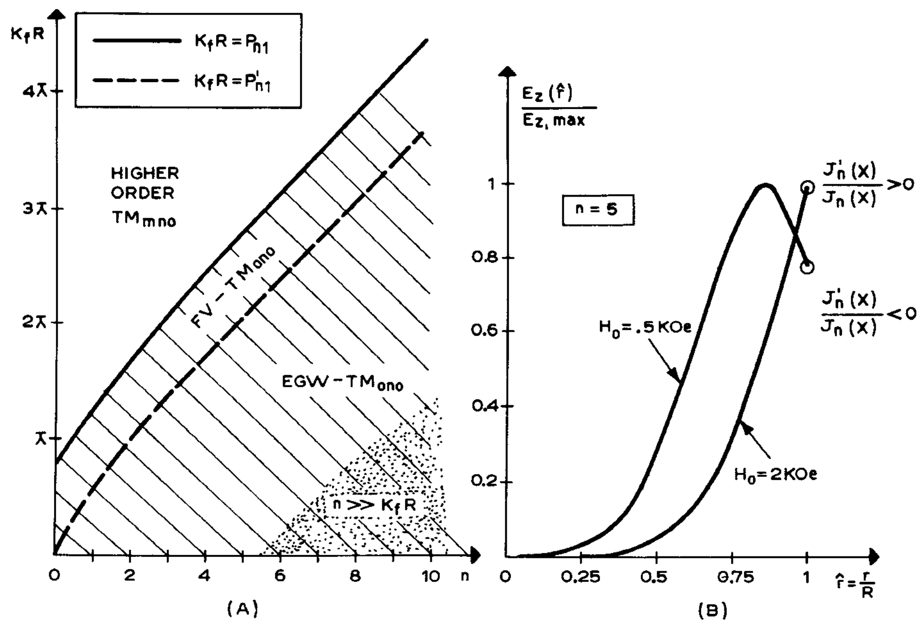

Fig. 5. (a) Existance regions of EGW–$TM_{0,n,0}$ modes on the k_yR versus coordinate plane. When $n \gg k_yR$, the EGW–$TM_{0,n,0}$ modes are strongly peaked at the disk's edge. (b) Calculated radial behavior of E_z normalized to $E_{z,\max}$ above ($H_0 = 2$ kOe) and below ($H_0 = 0.5$ kOe) the transition point ($n = 5$).

$TM_{0,n,0}$ modes exist for $0 < k_fR < p_{n1}'$ and FV–$TM_{0,n,0}$ modes exist for $p_{n1}' < k_fR < p_{n1}$. Here p_{n1}' indicates the first zero of J_n'.

This mode classification may be conveniently represented on a coordinate plane as shown in Fig. 5(a). In this figure, the shaded region represents the existence domain of the $TM_{0,n,0}$ modes. It is delimited by the continuous curve $k_fR = p_{n1}$ and is partitioned into two subregions by the dashed line $k_fR = p_{n1}'$. The blank region for $k_fR > p_{n1}$ is the existence domain of the higher order volume modes $TM_{m,n,0}$ ($m = 1,2,3,\cdots$). The pointed area represents the region where the inequality $n \gg k_fR$ is satisfied. In this region, EGW modes exist with $E_Z(r)$ strongly peaked at the disk's edge. In fact, when $n \gg k_fR$, $J_n(k_fR) \simeq [(k_fR)^n/n!\, 2^n]$ and

$$\frac{1}{k_f}\frac{d\hat{E}_Z(r)}{dr}\bigg|_{r=R} = \frac{J_n'(X)}{J_n} \simeq \frac{n}{X} \gg 1 \tag{13}$$

where the normalized quantity $\hat{E}_Z(r) = [E_Z(r)/E_Z(R)]$ has been used.

Let us now transfer these considerations to the mode chart of an actual ferrite MIC disk resonator (see Fig. 2). On a mode chart, if one traces along an n-constant curve (tuning curve) starting from high values of H_0, one finds EGW–$TM_{0,n,0}$ modes with a strong concentration of RF power at the disk's edge. Note the position of the $n \gg k_fR$

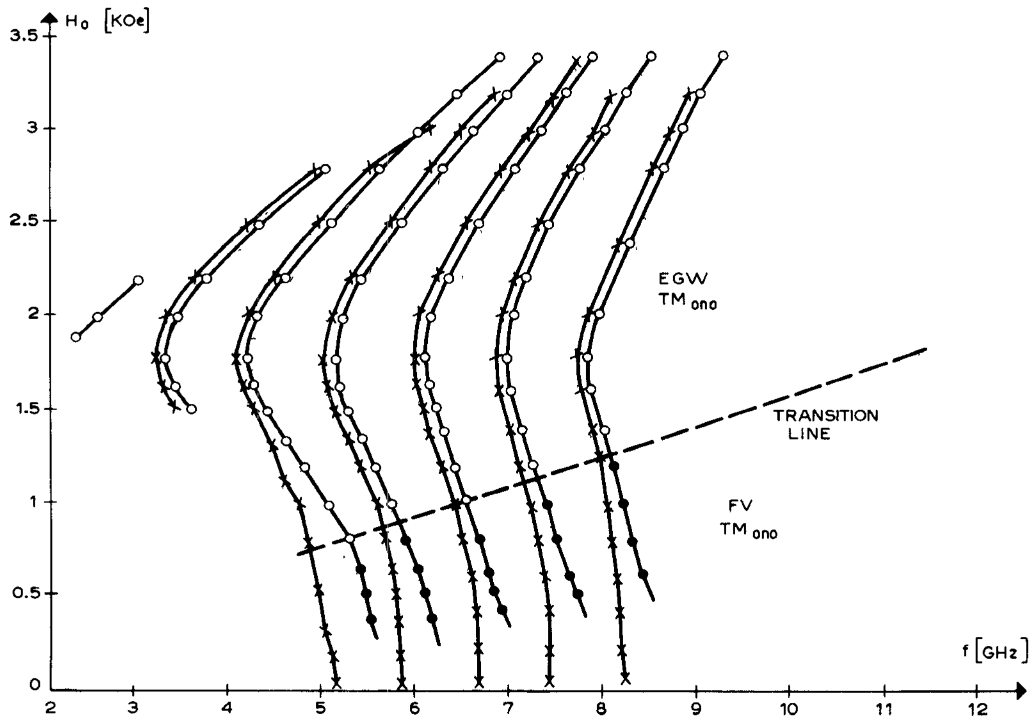

Fig. 6. Comparison between the mode chart of a disk resonator and a ring resonator.

region on the mode chart. As one moves toward lower values of H_0, one finds that the EGW character of the $TM_{0,n,0}$ modes maintains down to a point where $J_n'(X) = 0$. At this point, hereafter called "transition point," $E_Z(r)$ has a maximum at $r = R$ with a horizontal tangent $(dE_Z/dr)|_{r=R} = 0$. Crossing this point in the high-to-low H_0 direction, one finds that the maximum of $E_Z(r)$ detaches from the disk's edge and penetrates into the ferrite volume under the strip conductor. The EGW–$TM_{0,n,0}$ mode has transformed into an FV–$TM_{0,n,0}$ mode. In Fig. 2, we have indicated by an asterisk the various transition points. They were found by intersecting each experimental tuning curve with the $k_f R = p_{n1}'$ curve calculated for the same n. In Fig. 5(b), we have reported the behavior of $E_Z(r)/E_{Z,\max}$ calculated for two points, respectively, above and under a transition point ($n = 5$, $H_0 = 0.5$ and 2 kOe). Note how $[J_n'(X)/J_n(X)] > 0$ for an EGW mode while $[J_n'(X)/J_n(X)] < 0$ for an FV mode. As far as the position of the transition points on the mode chart is concerned, it may be recognized that it depends upon the particular law of variation assumed for $4\pi M$ as a function of H_0. The transition points of Fig. 2 were obtained for $4\pi M = H_0$. If one assumes a dependence of the type $4\pi M = (4\pi M_R)/(4\pi M_S)H_0$ [10], where $4\pi M_R = 1.25$ kOe is the remanence magnetization for YIG, the transition points locus is represented by the dashed curve in Fig. 2. Since no exact knowledge exists of $4\pi M(H_0)$, we tried to check the position of the transition points by experiment. Experiments were carried out on such a structure as an MIC ring resonator which would not perturb the EGW resonances but drastically affect the FV resonances. Fig. 6 shows the mode chart of a ring resonator having the same outer diameter as the disk's and a width of 0.6 mm. A comparison with the disk's results shows a considerable similarity in the EGW region and an increasing difference for decreasing values of H_0 where the disk's modes pick up a definite FV character. Unfortunately, an exact experimental determination of the transition points was not possible due to the gradual transformation of EGW modes into FV modes. Let us now demonstrate that the existence of the transition points in a magnetized ferrite MIC disk resonator is due to the fringing fields and that this information can be obtained directly from the characteristic equation (10). In fact, recognizing that in the present range of parameters $\mu_2/\mu_1 = -|\mu_2/\mu_1|$ and that

$$\frac{K_n'(\zeta)}{K_n(\zeta)} = -\left|\frac{K_n'(\zeta)}{K_n(\zeta)}\right|$$

the characteristic equation (10) may be recast in the form

$$X\frac{J_n'(X)}{J_n(X)} = -\frac{b}{b'}\mu_{\text{eff}}\zeta\left|\frac{K_n'(\zeta)}{K_n(\zeta)}\right| \mp n\left|\frac{\mu_2}{\mu_1}\right| \qquad (10')$$

where the plus and minus signs in front of n are, respectively, appropriate to an $\exp(jn\theta)$ or an $\exp(-jn\theta)$-dependence. From (10'), and recalling that $[J_n'(X)/J_n(X)]$ is either positive or negative, respectively, for EGW and FV–$TM_{0,n,0}$ modes, one draws the following conclusions. 1) For perfect magnetic-wall boundary conditions, $b/b' = 0$ and the results of Table I apply. Here one finds the well-known result that for $\exp(jn\theta)$, all the modes are FV, while for $\exp(-jn\theta)$ the modes are EGW. 2) In the presence of fringing fields, $b/b' > 0$ and the situation is represented in Table II. In this table, one sees that for one verse of azimuthal propagation, ($\exp jn\theta$), $TM_{0,n,0}$ modes are always FV. For the opposite sense, a transition occurs when

TABLE I
NATURE OF $TM_{0,n,0}$ MODES IN AN EGW DISK RESONATOR WITH PERFECT MAGNETIC-WALL BOUNDARY CONDITIONS

AZIMUTHAL DEPENDENCE	CHARACTERISTIC EQUATION	TYPE OF $TM_{o,n,o}$ MODE
exp (jnθ)	$\frac{J'_n(x)}{J_n(x)} = -\frac{n}{X}\left\|\frac{\mu_2}{\mu_1}\right\| < 0$	FV
exp(-jnθ)	$\frac{J'_n(x)}{J_n(x)} = \frac{n}{X}\left\|\frac{\mu_2}{\mu_1}\right\| > 0$	EGW

TABLE II
SAME AS IN TABLE I BUT WITH FRINGING-FIELD EFFECTS TAKEN INTO ACCOUNT

AZIMUTHAL DEPENDENCE	CHARACTERISTIC EQUATION		TYPE OF $TM_{o,n,o}$ MODE
exp (jnθ)	$\frac{J'_n(x)}{J_n(x)} = -D - \frac{n}{X}\left\|\frac{\mu_2}{\mu_1}\right\| < 0$; $D = \frac{b}{b'}\sqrt{\frac{\mu_{eff}}{\epsilon_f}}\left\|\frac{K'_n(\zeta)}{K_n(\zeta)}\right\|$		FV
exp(-jnθ)	$\frac{J'_n(x)}{J_n(x)} = -D + \frac{n}{X}\left\|\frac{\mu_2}{\mu_1}\right\|$	$\frac{n}{X}\left\|\frac{\mu_2}{\mu_1}\right\| > D$	EGW
		$\frac{n}{X}\left\|\frac{\mu_2}{\mu_1}\right\| = D$	TRANSITION
		$\frac{n}{X}\left\|\frac{\mu_2}{\mu_1}\right\| < D$	FV

TABLE III
NATURE OF $TM_{0,n,0}$ MODES IN A MIC DISK RESONATOR ON AN ISOTROPIC SUBSTRATE OF RELATIVE DIELECTRIC PERMITTIVITY ε_r AND MAGNETIC PERMEABILITY μ_r

	BOUNDARY CONDITION	CHARACTERISTIC EQUATION	TYPE OF $TM_{o,n,o}$ MODE
exp (±jnθ)	PERFECT MAGNETIC WALL	$\frac{J'_n(x)}{J_n(x)} = 0$	TRANSITION
	FRINGING FIELDS	$\frac{J'_n(x)}{J_n(x)} = -\frac{b}{b'}\sqrt{\frac{\mu_r}{\epsilon_r}}\left\|\frac{K'_n(\zeta)}{K_n(\zeta)}\right\|$	VOLUME

$J_n'(X) = 0$. 3) For $H_0 = 0$ (see Table III), one always finds volume modes and no EGW exist.

V. FRINGING-FIELD POWER

In Section III, it was shown that the fringing-field parameter b/b' can be determined by measuring the frequency spectrum of the resonator. Here we show how b/b' is related to the disk's edge admittance as seen from under the disk and how this quantity can be used to calculate the ratio of the reactive power stored in the fringing fields P_f to the RF power P_m contained within the ferrite volume under the strip conductor.

The total edge admittance Y_e, as seen from inside the ferrite under the disk, is found by recognizing that the boundary conditions at $r = R$ require

$$\frac{2\pi R H_{\theta f}(R)}{bE_{Zf}(R)} = Y_e. \tag{14}$$

Upon substituting (3) and (4) into (14), one finds

$$X\frac{J_n'(X)}{J_n(X)} \mp n\frac{\mu_2}{\mu_1} = j\frac{b}{2\pi} Y_e\mu_{\text{eff}}\frac{k_0}{Y_0} \tag{15}$$

which, when compared to (10), yields

$$Y_e = -jY_0\frac{2\pi R}{b}\frac{b}{b'}\frac{K_n'(\zeta)}{K_n(\zeta)}. \tag{16}$$

Once Y_e is known, the reactive power stored in the fringing fields is

$$P_f = \tfrac{1}{2}|Y_e|\,|E_{Zf}(R)|^2 b^2. \tag{17}$$

The RF power within the ferrite under the disk is

$$P_m = \pi b\omega\left[\mu_0\frac{\partial(\omega\mu_{\text{eff}})}{\partial\omega}\int_0^R (|H_{rf}|^2+|H_{\theta f}|^2)r\,dr - \varepsilon_0\varepsilon_f\int_0^R |E_{Zf}|^2 r\,dr\right]. \tag{18}$$

Upon substitution of (3)–(5) into (17) and (18), one finds

$$\frac{P_f}{P_m} = J_n^2(X)\left[\mu_{\text{eff}}\frac{b}{b'}\zeta\frac{K_n'(\zeta)}{K_n(\zeta)}\right] \cdot\left\{\left(1+\frac{\omega}{\mu_{\text{eff}}}\frac{\partial\mu_{\text{eff}}}{\partial\omega}\right)\left[\alpha\int_0^X\frac{J_n^2(t)}{t}\,dt + \beta\int_0^X J_{n-1}^2(t)t\,dt + \gamma\int_0^X J_n(t)J_{n-1}(t)\,dt - \int_0^X J_n^2(t)t\,dt\right]\right\}^{-2} \tag{19}$$

where t is a dummy variable and

$$\alpha = 2n^2\left(\frac{\mu_2}{\mu_1}\pm 1\right)^2$$

$$\beta = 1+\left(\frac{\mu_2}{\mu_1}\right)^2$$

$$\gamma = -\frac{\alpha}{n}.$$

The integrals in (19) are solved as follows [11]:

$$\int_0^X J_n^2(t)t\,dt = \frac{X^2}{2}\left[J_n^2(X) - J_{n-1}(X)J_{n+1}(X)\right] \tag{20}$$

$$\int_0^X \frac{J_n^2(t)}{t}\,dt = \sum_{r=0}^{\infty}\frac{(-1)^r(2n+2r-1)!}{r!(2n+r)![(n+r)!]^2}\left(\frac{t}{2}\right)^{2(n+r)} \tag{21}$$

$$\int_0^X J_n(t)J_{n-1}(t)\,dt = \sum_{r=0}^{\infty}\frac{(-1)^r(2n+2r-1)!}{r!(2n-1+r)![(n+r)!]^2}\left(\frac{t}{2}\right)^{2(n+r)}. \tag{22}$$

Numerical computations using formula (19) revealed that in the disk under consideration the ratio P_e/P_m is of the order of a few percents when $b/b' = 0.5$. Note that formula (19) is also applicable to MIC disk resonators of smaller diameter, such as are used in the traditional Y-junction MIC circulators.

VI. Conclusions

A study has been presented of the $TM_{0,n,0}$ modes in ferrite MIC disk resonators of large diameter magnetized perpendicularly to the ground plane. Fringing-field effects have been included in the analysis via a semiempirical equivalent model. A fringing-field parameter b/b' has been introduced which allows one to predict the correct mode chart of a disk resonator. Numerical values of b/b' have been determined at C and X band for a dc magnetic field ranging from 0 to 3.5 kOe. Transition points have been found on the mode chart of the resonator where EGW modes transform into FV modes. Fringing fields are found to be responsible for the existence of these points. Finally, the ratio of the fringing field's power to the RF power stored within the ferrite under the strip conductor is determined as a function of the fringing-field parameter b/b'.

References

[1] G. Cortucci and P. de Santis, "Fringing field effects in edge-guided wave circuits," in *Proc. 1975 European Microwave Conf.*, pp. 283–287.
[2] L. K. Brundle, "Experimental study of magnetodynamic edge-guided waves on a microwave ferrite substrate," *IEEE Trans. Magn.*, vol. MAG-11, pp. 1282–1284, Sept. 1975.
[3] M. E. Hines, "Reciprocal and non-reciprocal modes of propagation in ferrite strip line and microstrip devices," *IEEE Trans. Microwave Theory Tech.*, vol. MTT-19, pp. 442–451, May 1971.
[4] P. de Santis, "Edge guided modes in ferrite microstrips with curved edges," *Appl. Phys.*, vol. 4, pp. 167–174, July 1974.
[5] W. J. Getsinger, "Microstrip dispersion model," *IEEE Trans. Microwave Theory Tech.*, vol. MTT-21, pp. 34–39, Jan. 1973.
[6] S. A. Schelkunoff, *Electromagnetic Waves* New York: Van Nostrand, 1943, p. 261.
[7] H. Bosma, "On strip line Y-circulators at UHF," *IEEE Trans. Microwave Theory Tech.*, vol. MTT-12, pp. 61–72, Jan. 1964.
[8] J. J. Green and F. Sandy, "Microwave characterization of partially magnetized ferrites," *IEEE Trans. Microwave Theory Tech.*, vol. MTT-22, pp. 641–645, 1974.
[9] H. D. Rüpke, "Magnetodynamic modes in ferrite spheres for microwave filter applications," *IEEE Trans. Magn.*, vol. MAG-6, pp. 80–84, Mar. 1970.
[10] T. Miura and T. Hashimoto, "Comments on 'A new concept for broad banding the ferrite substrate circulator based on experimental modal analysis,'" *IEEE Trans. Microwave Theory Tech.*, vol. MTT-21, pp. 71–74, Jan. 1974.
[11] N. W. McLachlan, *Bessel functions for Engineers*, 2nd ed. Oxford: Oxford University Press, 1955, p. 63.

Experimental Measurement of Microstrip Transistor-Package Parasitic Reactances

ROBERT J. AKELLO, MEMBER, IEEE, BRIAN EASTER, MEMBER, IEEE, AND I. M. STEPHENSON

***Abstract*—A resonance method of measurement is described for the determination of the parasitic reactances of a microwave transistor package mounted in microstrip. Results for two types of package obtained from normal-sized and from scaled-up models are presented. The influence of the parasitics on the characteristics of a typical microwave FET chip is briefly discussed.**

I. Introduction

THE parasitic reactances associated with the package or mounting can seriously limit the performance of a microwave semiconductor device and need to be accurately known for good circuit and device modeling. Some diode packages in coaxial mounts, such as the S4 have been examined thoroughly [1], [2], but relatively sparse data are available on packages for microstrip application [3], [12]. The rapid advance in the performance of gallium arsenide FET's highlights the need for the accurate characterization and improvement of packages and mountings suitable for hybrid MIC's. In this paper two types of transistor packages will be considered, the leadless inverted device (LID) and the S2 package proposed by James *et al.* [4].

Manuscript received June 2, 1976; revised October 4, 1976.
The authors are with the School of Electronic Engineering Science, University College of North Wales, Dean Street, Bangor, Caerns, Wales, Great Britain.

Previous papers [5]–[7] have described the measurement of the small reactances and susceptances of microstrip junctions and discontinuities, using a resonance technique and a close approach to a substitution procedure. In this procedure the change in resonant frequency is observed when the unknown element is introduced into a microstrip resonant circuit, only light coupling through noncritical connections being required for accurate determination of resonance. This method has the advantage of largely avoiding the problems entailed in the measurement of microstrip circuits through a coaxial-to-microstrip transition. While this approach often cannot be directly used for active devices, due to the low-circuit Q-factor that would result, it can be usefully applied to the study of the package parasitics. In addition to examining normal-sized packages with the active element appropriately disabled or disconnected, the method has been used to study scaled-up models of the package and circuit, Stycast material of the correct permittivity being employed in place of the ceramics of the package and circuit substrate. This is a quick and accurate method